doi:10.1093/brain/awr146 Brain 2011: 134; 1943–1958 | 1943

BRAIN
A JOURNAL OF NEUROLOGY

Neuronal expression of TATA box-binding protein containing expanded polyglutamine in knock-in mice reduces chaperone protein response by impairing the function of nuclear factor-Y transcription factor

Shanshan Huang, Joseph J. Ling, Su Yang, Xiao-Jiang Li and Shihua Li

Department of Human Genetics, Emory University, Atlanta, GA 30322, USA

Correspondence to: Xiao-Jiang Li,
Department of Human Genetics,
Emory University,
615 Michael St 347,
Atlanta, Georgia 30322,
USA
E-mail: xli2@emory.edu

Correspondence may also be addressed to: Shihua Li. E-mail: sli@emory.edu

The polyglutamine diseases consist of nine neurodegenerative disorders including spinocerebellar ataxia type 17 that is caused by a polyglutamine tract expansion in the TATA box-binding protein. In all polyglutamine diseases, polyglutamine-expanded proteins are ubiquitously expressed throughout the body but cause selective neurodegeneration. Understanding the specific effects of polyglutamine-expanded proteins, when expressed at the endogenous levels, in neurons is important for unravelling the pathogenesis of polyglutamine diseases. However, addressing this important issue using mouse models that either overly or ubiquitously express mutant polyglutamine proteins in the brain and body has proved difficult. To investigate the pathogenesis of spinocerebellar ataxia 17, we generated a conditional knock-in mouse model that expresses one copy of the mutant TATA box-binding protein gene, which encodes a 105-glutamine repeat, selectively in neuronal cells at the endogenous level. Neuronal expression of mutant TATA box-binding protein causes age-dependent neurological symptoms in mice and the degeneration of cerebellar Purkinje cells. Mutant TATA box-binding protein binds more tightly to the transcription factor nuclear factor-Y, inhibits its association with the chaperone protein promoter, as well as the promoter activity and reduces the expression of the chaperones Hsp70, Hsp25 and HspA5, and their response to stress. These findings demonstrate how mutant TATA box-binding protein at the endogenous level affects neuronal function, with important implications for the pathogenesis and treatment of polyglutamine diseases.

Keywords: polyglutamine; transcription factor; neurodegeneration; ataxia; animal models

Abbreviations: HEK293 = human embryonic kidney 293 cell line; HSP = heat shock protein; SCA17 = spinocerebellar ataxia type 17; TBP = TATA box-binding protein

Received March 9, 2011. Revised April 23, 2011. Accepted May 13, 2011

Introduction

Polyglutamine expansion in various proteins causes nine inherited neurodegenerative diseases, including Huntington's disease, dentatorubral-pallidoluysian atrophy (DRPLA), spinal bulbar muscular atrophy, and spinocerebellar ataxia types 1, 2, 3, 6, 7 and 17 (Orr and Zoghbi, 2007). The common feature of these diseases is selective neurodegeneration in the brain, despite the widespread expression of the disease proteins throughout the body. It is evident that polyglutamine expansion causes proteins to misfold and abnormally interact with other proteins to mediate neuropathology. We also know that the normal function of polyglutamine proteins can contribute to or modulate neuropathology (Duvick *et al*., 2010). Of the nine polyglutamine diseases, spinocerebellar ataxia type 17 (SCA17) is caused by polyglutamine expansion (>43 glutamines) in the TATA box-binding protein (TBP) (Koide *et al*., 1999; Nakamura *et al*., 2001), which is an essential transcription factor for the expression of most genes. Like other polyglutamine diseases, SCA17 shows late-onset neurodegeneration that is particularly prominent in the cerebellum (Koide *et al*., 1999; Nakamura *et al*., 2001; Rolfs *et al*., 2003; Bauer *et al*., 2004; Bruni *et al*., 2004; Toyoshima *et al*., 2004). Of all identified polyglutamine proteins, TBP is the smallest and has been well characterized for its function. Thus, SCA17 makes an ideal disease model for understanding how polyglutamine expansion alters the function of TBP and causes selective neuropathology, which would have important implications for understanding the pathogenesis of polyglutamine diseases.

There are various mouse models of polyglutamine diseases that provide mechanistic insight into polyglutamine disease pathology, and a variety of pathological pathways have been uncovered or proposed from studies of different polyglutamine animal models. What has become clear is that the expression levels of mutant genes and the protein context are critical for the neurological phenotypes and pathological events identified. For example, transgenic mice overexpressing small mutant N-terminal huntingtin fragments can develop more progressive and robust phenotypes than those mice that express full-length mutant huntingtin (Menalled and Chesselet, 2002; Heng *et al*., 2008). Also, glia–neuron interactions and the non-neuronal toxicity of polyglutamine disease proteins contribute to polyglutamine disease neuropathology (Bradford *et al*., 2009; 2010; Sassone *et al*., 2009; van der Burg *et al*., 2009). Given that selective neurodegeneration is a characteristic of all polyglutamine diseases, it would be interesting to know the specific effect of mutant proteins on neuronal function. Current polyglutamine disease models were generated either by overexpressing mutant proteins in neuronal cells or ubiquitously expressing mutant proteins in all types of cells, making it difficult to define the specific effect of endogenous mutant protein in neurons.

Because the overexpression of misfolded proteins could impair cellular homeostasis and the capacity for removing toxic proteins and therefore may confound the proposed mechanisms and pathogenesis of diseases, identifying the selective neuronal effects of mutant polyglutamine proteins when they are expressed at the endogenous levels is key. To this end, we established a new mouse model that selectively expresses mutant TBP in neuronal cells at the endogenous level. This mouse model exhibited age-dependent and progressive neurological symptoms and neurodegeneration. We show that mutant TBP abnormally interacts with the transcription factor nuclear factor-YA and affects its transcriptional activity on the expression of chaperone proteins. As a result, mutant TBP at the endogenous level can impair the expression of several chaperone proteins and their response to stress. Since chaperone proteins are protective against misfolded proteins and oxidative stress, our findings suggest that mutant TBP affects neuronal function by impairing chaperone protein levels, offering a new therapeutic target.

Materials and methods

Antibodies and reagents

Rabbit polyclonal antibody against C-terminal amino acids 204–259 of mouse TBP was generated in our previous study (Friedman *et al*., 2007). Other antibodies were obtained from commercial sources for the following antigens: the N-terminal 1–20 amino acids of TBP (1TBP18, Fisher Scientific), expanded polyglutamine (1C2, Millipore/Chemicon), nuclear factor-YA (H209, Santa Cruz Biotechnology), heat shock protein HSP27/25 (C20, Santa Cruz Biotechnology), HSP70 (W27, Santa Cruz Biotechnology), HSPA5 (C20, Santa Cruz Biotechnology), calbindin (Millipore/Chemicon), γ-tubulin (GTU-88, Sigma) and GAPDH (Millipore/Chemicon). Hoechst 33 258 (Invitrogen/Molecular Probes) was used for nuclear labelling. Secondary antibodies were donkey anti-mouse or donkey anti-rabbit antibodies that were purchased from Jackson Immunoresearch. Alexa fluorescence-labelled secondary antibodies were purchased from Invitrogen. Transfections were performed with Lipofectamine 2000 (Invitrogen). Full-length *TBP* complementary DNA constructs encoding CAG/polyglutamine tracts of different lengths (13, 71 and 105 CAGs) were described previously (Friedman *et al*., 2007).

Mice

Transgenic SCA17 mice were generated as described previously (Friedman *et al*., 2007). To generate nestin-TBP knock-in mice, we cloned a mouse TBP genomic fragment containing exons 1 and 2 and replaced exon 2 of the mouse TBP gene with human TBP exon 2 carrying 105 CAGs. A DNA cassette containing three stop codons was inserted in the front of the initiation site of this mouse TBP gene carrying 105 CAGs. The stop codons are flanked by two loxP sites in a targeting vector. The targeting vector was linearized prior to electroporation into 129SvEv embryonic stem cells. Positive embryonic stem cells containing targeted vectors were identified by genomic DNA polymerase chain reaction and Southern blotting, and then injected into C57B1/6J blastocysts to generate chimeric mice by inGenious Targeting Laboratory, Inc. Chimeric males were crossed with wild-type mice (C57BL/6) to generate heterozygous floxed (*TBP-105 glutamine*$^{+/loxp}$) mice. The floxed mice were crossed with mice carrying a nestin promoter-driven *Cre* transgene [The Jackson Laboratory, B6.Cg (SJL)-TgN(NesCre)1Kln], which expresses Cre primarily in the CNS and PNS under the control of the rat nestin promoter and enhancer (Tronche *et al*., 1999). Floxed

heterozygous mice without Cre live normally as wild-type mice and were used as a control to compare with those floxed mice that also express Cre and mutant TBP (nestin-TBP knock-in) in neuronal cells. All mice were bred and maintained in the animal facility at Emory University under specific pathogen-free conditions in accordance with institutional guidelines of The Animal Care and Use Committee at Emory University. Primers with sequences flanking the TBP CAG/CAA repeat and of Cre DNA sequence were used for polymerase chain reaction genotyping. The sequences of the forward and reverse primers for mutant TBP are as follows: (forward: 5′-CCA CAG CCT ATT CAG AAC ACC-3′; reverse: 5′-AGA AGC TGG TGT GGC AGG AGT GAT-3′). The sequences of the forward and reverse primers for Cre are as follows: forward: (5′-GCGGTCTGGCAGTAAAAACTATC-3′) and reverse: (5′-TGTTTCACTATCCAGGTTACGG-3′).

Cell culture

Human embryonic kidney (HEK) 293 cells were cultured in Dulbecco's modified Eagle's medium supplemented with 10% foetal bovine serum, 100 U/ ml penicillin and 100 mg/ml streptomycin. Cerebellar granule neurons were cultured from postnatal (P5-P9) transgenic SCA17 mice as described previously (Friedman *et al*., 2007, 2008). After culturing for 15 days *in vitro*, cerebellar neurons were fixed with 4% paraformaldehyde and stained with TBP and nuclear factor-YA antibodies. The stable PC12 cell lines were generated as previously described (Friedman *et al*., 2007; Shah *et al*., 2009). The cell lines were cultured in Dulbecco's modified Eagle's medium supplemented with 10% horse serum, 5% foetal bovine serum and 1% penicillin/streptomycin (Invitrogen).

Western blot analysis and immunohistochemistry

For western blots, cultured cells or brain tissues were homogenized in RIPA buffer (50 mM Tris, pH 8.0, 150 mM NaCl, 1 mM ethylenediaminetetraacetic acid pH 8.0, 1 mM ethylene glycol tetraacetic acid, pH 8.0, 0.1% sodium dodecyl sulphate, 0.5% deoxycholate and 1% Triton X-100) with 1× protease inhibitor from Sigma (P8340) or Pierce (78438). The cell or tissue lysates were diluted in 1× sodium dodecyl sulphate sample buffer (62.6 mM Tris–HCl, pH 6.8, 2% sodium dodecyl sulphate, 10% glycerol and 0.01% bromophenol blue) and sonicated for 10 s after incubation at 100°C for 5 min. The total lysates (50 μg) were resolved in a Tris–glycine gel (Invitrogen) and blotted to a nitrocellulose membrane (Hybond ECL GE Health Care/Amersham Biosciences). The western blots were developed using the ECL Plus Chemiluminescence kit (GE Health Care/Amersham Biosciences).

Immunofluorescence and immunohistochemistry were performed as previously described (Friedman *et al*., 2007; Shah *et al*., 2009). When the 1TBP18 antibody was used for immunocytochemistry, fixed brain sections were treated with 88% formic acid for 10 min prior to incubation with 1TBP18 at 1:1000 dilution. Light micrographs were taken using a Zeiss microscope (Axiovert 200 MOT) and a ×63 lens (LD-Achroplan ×63/0.75) with a digital camera (Hamamatsu Orca-100) and OpenLAB software. Fluorescent images were acquired on a Zeiss microscope (Axiovert 200 MOT; Carl Zeiss Imaging) equipped with a digital camera (Hamamatsu Orca-100) and OpenLAB software (Improvision Inc). Both ×20 and ×63 objectives were used for image acquisition.

Behavioural analysis

Mouse body weight and growth were measured monthly. The motor function of mice was assessed using a rotarod test (AccuScan Instruments Inc). Rotarod performance was evaluated as previously described (Friedman *et al*., 2007). Mice were trained for 5 min on two separate days on a rod that rotated at 5 rpm. Testing commenced the following week on a rod that rotated at 15 rpm. Mice were subjected to three trials, each with a maximum duration of 180 s and latency to fall was recorded. Mice were tested monthly at the same time of day. Locomotor activity was assessed with an automated system (San Diego Instruments) with photobeams that recorded ambulations (consecutive beam breaks). Mice were placed individually in the chambers with free access to food and water in a 12-h light (0700–1900 h) and 12-h dark (1900–0700 h) cycle. Mice were allowed to acclimate for 3 h before recording. Activity was recorded once per hour. Nest building and utilization were assessed as previously described (Moretti *et al*., 2005) with some modifications. A nest block was placed into the cage of individually housed mice, and the nest building was monitored by measuring the nest quality at 1, 2 and 24 h using the following scale: (0) nesting material unmodified; (1) flat nest with partially shredded nesting material; (2) shallow nest with shredded material, but lacking fully formed walls; (3) nest with well-developed walls; (4) nest in the shape of a cocoon with partial or complete roof; and (5) nest in a good shape and with a complete roof.

Protein interaction studies

For *in vitro* GST pulldown, GST-tagged TBP complementary DNAs encoding 13- or 71-glutamine were subcloned into the PGEX-4T-2 vector. Recombinant proteins were expressed in *E. coli* BL21 (DE3) by induction with 1 mM isopropyl D-thiogalactopyranoside for 1.5 h at room temperature. GST fusion proteins were purified with glutathione agarose beads (Sigma). Human nuclear factor-YA complementary DNA was obtained by reverse transcriptase-polymerase chain reaction using sense primer 5′-CTA TCG ATG AGG GAC CAT GGA GCA GTA TAC AGC-3′ and antisense primer 5′-GGA ATT CGG ACA CTC GGA TGA TCT GTG-3′, verified by sequencing, and inserted to the pRK5 vector. *In vitro* translated nuclear factor-YA was obtained from PRK-nuclear factor-YA construct using the TNT *in vitro* translation kit (Promega). Following translation, equal amounts (3–4 μl) of *in vitro* synthesized nuclear factor-YA were diluted in 150 μl of GST protein binding buffer [0.3% TritonX-100/0.05M phosphate-buffered saline with PMSF (phenylmethylsulphonyl fluoride) and protease inhibitors] and incubated for 2 h at 4°C with GST-TBP fusion proteins attached to glutathione-conjugated beads. The beads were pelleted by centrifugation, washed three times in GST buffer, boiled in sodium dodecyl sulphate sample buffer and resolved on a sodium dodecyl sulphate–polyacrylamide gel. For immunoprecipitation of transfected proteins in HEK293 cells, we used anti-nuclear factor-YA or purified rabbit immunoglobulin G (IgG, 1 μg, Jackson Immonoresearch) to precipitate extracts from HEK293 cells cotransfected with nuclear factor-YA and TBP containing 31- or 71-glutamine. For immunoprecipitation of brain cerebellar extracts, we used anti-TBP (EM192) or purified rabbit IgG to precipitate mouse cerebellar extracts. Immunocomplexes were allowed to form overnight at 4°C and then precipitated with protein A-agarose (20 μl, 1:1 dilution, Sigma) for 1 h. Input in western blot was 5% (cells) or 12.5% (brain tissue) of lysates for immunoprecipitation.

Luciferase promoter activity assay

The human HSP27 promoter containing CCAAT (−1903 to −1598, minimal promoter) and proximal (−2103 to −1598) regions were isolated from genomic DNA using polymerase chain reaction with the sense primers 5′-GGA AAG CTT GCT CGG TCA TGC TGG-3′ (proximal), 5′-GAG AAG CTT GCG AAG AGG GTT CAG C-3′ (minimal) and antisense primer 5′-GGG GTA CCG TGG TGA GAT CAT AGC-3′. The isolated promoter DNAs were inserted into the pGL4.14 reporter vector (Promega) using HindIII and KpnI restriction sites. Reporter constructs were cotransfected with the indicated expression vectors into HEK293 cells. ONE-Glo™ Luciferase Assay System reagent (Promega) was used to detect reporter activity with a FLUOstar Galaxy luminescence plate reader (BMG Labtechnologies).

Chromatin immunoprecipitation

Chromatin immunoprecipitation assays with semi-quantitative polymerase chain reaction were performed as previously described (Friedman *et al*., 2007; Shah *et al*., 2009). HEK293 cells were transfected with TBP (13-glutamine or 105-glutamine) and nuclear factor-YA constructs and collected 48 h after transfection. For each immunoprecipitation, 850 μg of cell lysate was used with or without 5 μg of anti-nuclear factor-YA. Semi-quantitative polymerase chain reaction, using human β-actin and HSP27 primers in separate reactions, was performed on DNA recovered from immunoprecipitated samples and inputs (10% pre-clarified lysate). Polymerase chain reaction without template DNA served as negative controls. Promoter sequences were acquired using the UCSC genome browser to include nuclear factor-YA binding sites. The size of the amplicons for β-actin and HSP27 were 123 and 89 bp, respectively. Primer sequences and polymerase chain reaction cycling parameters were as follows: human β-actin: sense 5′-AAT CCT GCA CTG TCG GCG AAG C-3′and antisense 5′-CGC GCC GCT GGG TTT TAT AGG G-3′, human HSP27: sense 5′-CTA TCT CAC ACG CGT GTG GTT CC-3′ and antisense 5′-TTA AGG AGG ACA GAG CCA GAC AG-3′. Polymerase chain reaction conditions were as follows: 96°C for 3 min, 96°C for 45 s, 58°C for 45 s and 72°C for 45 s with 30 cycles. Polymerase chain reaction products were electrophoresed on a 2.2% agarose gel. Densitometry was used to measure polymerase chain reaction product signals from the precipitates after subtracting the background signals from the precipitates in the absence of anti-nuclear factor-YA antibody. The ratios of the precipitated polymerase chain reaction products to input were then calculated.

Heat shock and hydrogen peroxide treatment

TBP stably transfected PC12 cells were seeded 24 h prior to treatment. To induce heat shock proteins, cells were transferred to 42°C, 5% CO_2 in a humidified incubator for 45 min, then recovered at 37°C for 4, 8 and 16 h. To stress cells with H_2O_2, cells were treated with H_2O_2 as described previously (Pan *et al*. 2010) with some modification. Cells were exposed to 50, 100 and 250 μM H_2O_2 for 4 h. At the end of treatment, the cells were washed twice with warm medium and continuously cultured in normal medium for 8 h at 37°C.

For mouse heat shock treatment, 2-month-old mice were maintained on a light/dark (12 h/12 h) cycle at 23°C and received food and water. All procedures were performed according to protocols approved by the Institutional Committee for Use and Care of Laboratory Animals. The procedure for heat stress in the present study was similar to that described previously (Hu *et al*. 1997). Briefly, exposure to elevated temperature was achieved by placing mice in a positive forced air incubator for 1 h at 45°C. Following heat stress, mice were recovered at room temperature for 16 h, and then sacrificed for isolating brain tissues.

Statistical analysis

Results generated from three or more independent experiments are expressed as the mean ± SE and were analysed for statistical significance using GraphPad Prism 5 software. Differences were considered statistically significant with a $P < 0.05$.

Results

Generation of conditional SCA17 mice that express mutant TBP in neuronal cells

To generate a mouse model that could selectively express mutant TBP in neuronal cells, we inserted a stop codon in front of the initiation site of the mutant mouse TBP gene that encodes a 105-CAG/glutamine repeat. This mutant mouse TBP gene was generated by replacing exon 2 of the mouse TBP gene with human TBP exon 2 carrying 105 CAGs. The stop codon is flanked by two loxP sites in a targeting vector and can be removed by Cre recombination. Heterozygous mice that have one copy of the mutant TBP gene were generated using a standard gene targeting approach that involves the selection of embryonic stem cells containing the targeted TBP gene. The heterozygous floxed mice carrying one copy of the targeted TBP gene are equivalent to heterozygous TBP knockout mice, which are viable and grow normally as wild-type mice (Martianov *et al*., 2002). The heterozygous floxed TBP knock-in mice were mated with transgenic mice expressing Cre under the control of the rat neuronal nestin promoter (Tronche *et al*., 1999). The stop codon in the crossed mice was removed via Cre–loxP recombination, resulting in SCA-17 knock-in mice (nestin-TBP knock-in) that express both mutant and normal TBP under the endogenous promoter in neuronal cells (Fig. 1A).

To verify the expression of mutant TBP in nestin-TBP knock-in mice, we performed western blot analysis of brain extracts from nestin-TBP knock-in mice on postnatal Days 2–30. Probing the western blot with an antibody to expanded polyglutamine (1C2) revealed the presence of soluble mutant TBP in nestin-TBP knock-in mice, but not in heterozygous floxed mice without Cre expression, indicating that Cre expression under the nestin promoter leads to the expression of mutant TBP expression (Fig. 1B). Western blotting with the 1TBP18 antibody, which is against the N-terminal region of TBP and can preferentially react with polyglutamine-expanded TBP (Friedman *et al*., 2007), revealed aggregated TBP that remained in the stacking gel (Fig. 1C). We also performed 1TBP18 immunohistochemistry to verify the expression of mutant TBP in nestin-TBP knock-in mice. Mutant TBP is distributed in various brain regions, including the cortex, striatum, brain stem and cerebellum. Positive staining appeared to be restricted to the grey matter, but not the white

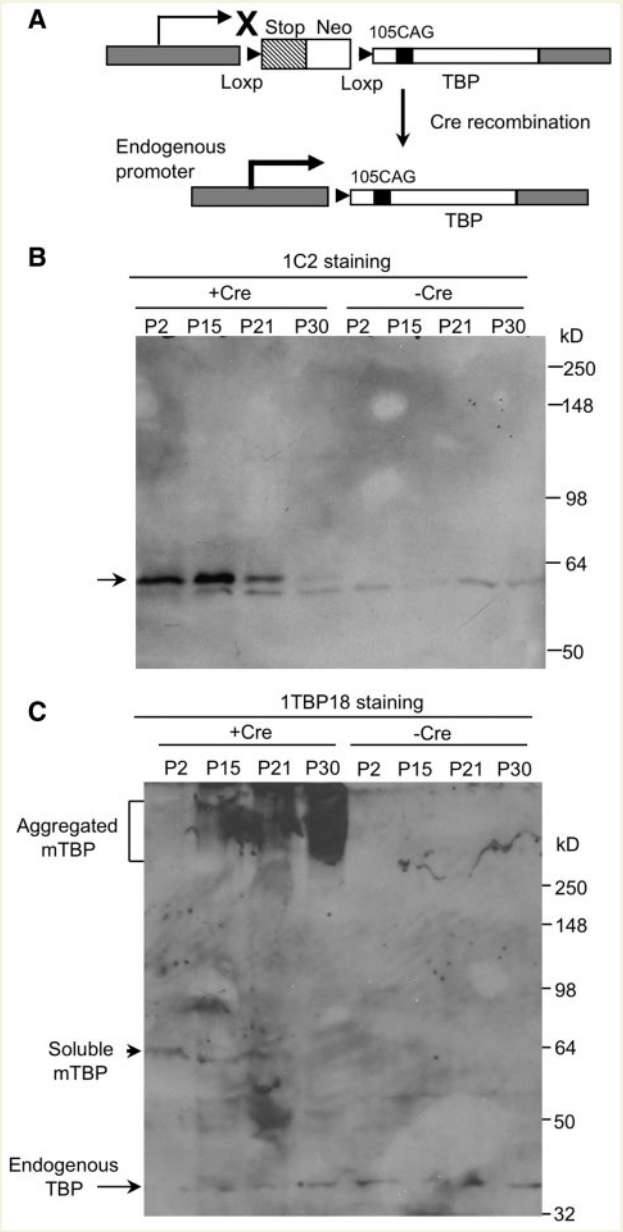

Figure 1 Expression of mutant TBP in nestin-TBP knock-in mice. (**A**) The schematic structure of the targeted mouse TBP gene, which has a stop codon and the neomycin (Neo) resistance gene flanked by two loxP sites to prevent the transcription of the mutant TBP gene. After Cre recombination, the stop codon and Neo resistance gene are removed, leading to the expression of the mutant TBP gene with 105 CAGs. (**B**) TBP western blot of cerebellar lysates from nestin-TBP knock-in mice with Cre recombinase (+Cre) or floxed nestin-TBP mice without Cre (−Cre). Lysates were from the cerebellum of mice at postnatal (P) 2–30 days. The blot was probed with 1C2 antibody that is against expanded polyglutamine. Arrow indicates soluble mutant TBP-105-glutamine protein. (**C**) The same blot was probed with 1TBP18 antibody that is against N-terminal TBP. Arrow indicates endogenous TBP, arrowhead indicates soluble mutant TBP-105-glutamine (mTBP) protein, and square bracket indicates aggregated TBP.

matter, consistent with the neuronal expression pattern under the nestin promoter (Fig. 2A). High magnification micrographs showed that mutant TBP was largely diffuse in the nuclei of neuronal cells in different brain regions (Fig. 2B). This diffuse staining was seen in mice from the ages of 4–22 months, suggesting that mutant TBP, when expressed at the endogenous level, does not form large nuclear inclusions as seen in transgenic mice that overexpress mutant TBP under the control of the prion promoter (Friedman *et al*., 2007). Consistently, staining with an antibody to ubiquitin failed to reveal nuclear aggregates (Supplementary Fig. 1A). However, we saw small nuclear aggregates in cerebellar Purkinje cells in nestin-TBP knock-in mice. Because western blots clearly demonstrated aggregation of mutant TBP, aggregates formed by mutant TBP in nestin-TBP knock-in mice could be small or their antigenicity could have been masked for the antibodies we used in immunohistochemistry.

Age-dependent neurological phenotypes and neurodegeneration in nestin-TBP mice

Nestin-TBP knock-in mice developed an age-dependent neurological symptom with an obvious hunchback appearance and reduced body size at 22 months of age (Fig. 3A). They started to gain less body weight after 12 months, a phenomenon that was more prominent in male nestin-TBP knock-in mice (Fig. 3B). Rotarod performance, which reflects the motor function of mice, was decreased in nestin-TBP knock-in mice compared with the littermate controls, and we saw a significant decrease in female nestin-TBP knock-in mice older than 12 months (Fig. 3C). However, these phenotypes are milder and occur much later than those of transgenic mice that overexpress mutant TBP by the mouse prion promoter (Friedman *et al*., 2007), suggesting that the expression level of mutant TBP is critical for the extent of neurological phenotypes.

We also examined the locomotor activity of nestin-TBP knock-in mice and observed that their locomotor activity is reduced at night (Fig. 3D) at a later stage. The relative decrease in activity in the dark phase is largely due to reduced locomotion (Moretti *et al*., 2005). Another noticeable phenotype in nestin-TBP knock-in mice is their reduced nest-building behaviour. Nestin-TBP knock-in mice were unable to build nests, which is evident from the presence of largely untouched nesting material (Fig. 3E). Nest-building behaviour represents a form of home-cage activity that is often linked to social behaviour and can be impacted by considerable global motor coordination impairments (Szczypka *et al*., 2001; Ballard *et al*., 2002) and non-motor social interaction defects (Sluyter *et al*., 1995; Lijam *et al*., 1997; Long *et al*., 2004; Moretti *et al*., 2005). Both male and female nestin-TBP knock-in mice, regardless of their ages, showed significant difficulty in nest-building activity (Fig. 3F). Thus, expression of mutant TBP in neuronal cells in nestin-TBP knock-in mice apparently causes neurological and social interaction abnormalities, consistent with the clinical symptoms of human patients with SCA17 (Zühlke *et al*., 2003; Mariotti *et al*., 2007).

The main pathological characteristic of SCA17 is the predominant degeneration of the cerebellum cells, especially Purkinje cells

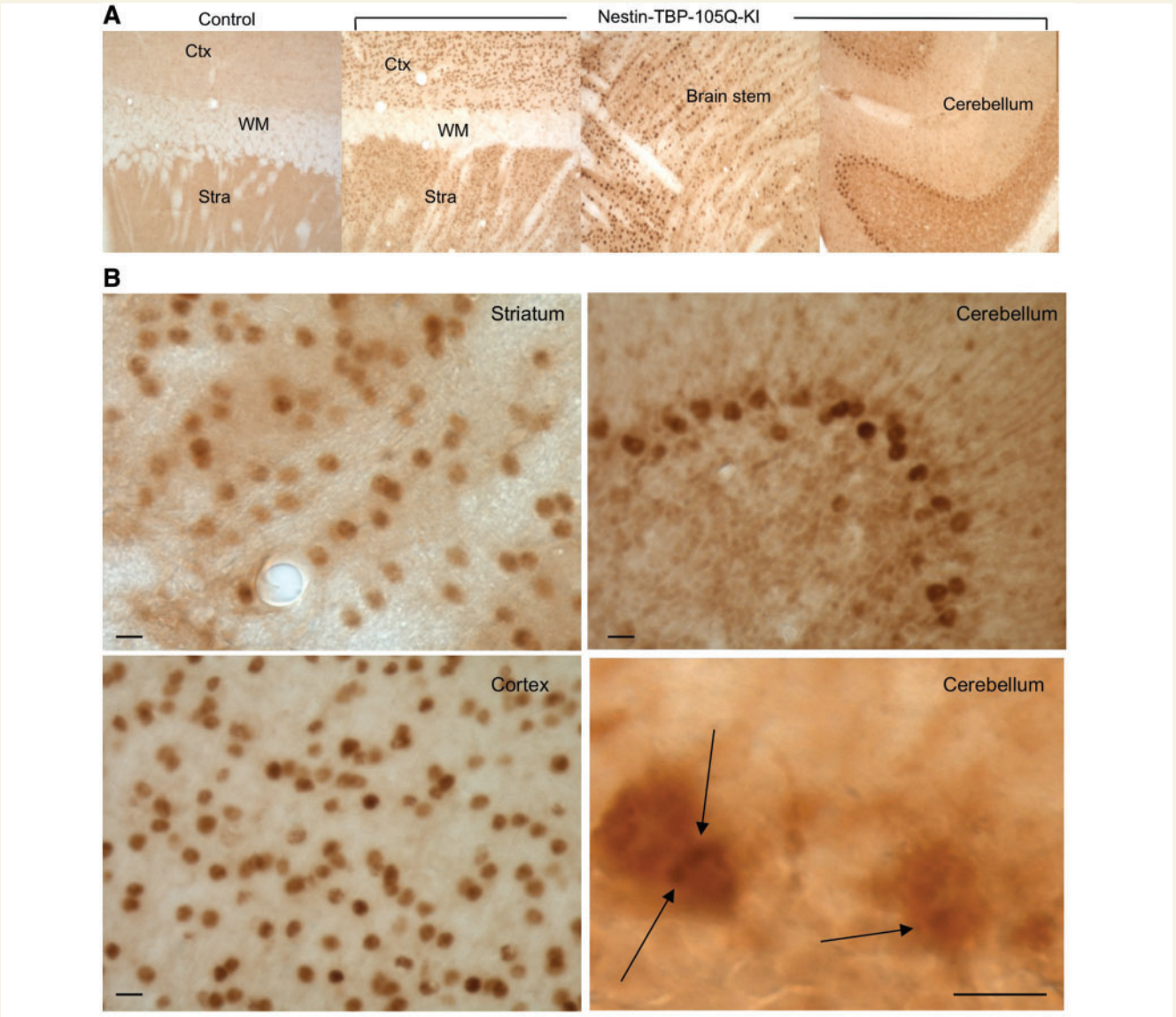

Figure 2 The distribution of mutant TBP in nestin-TBP knock-in mouse brain. (**A**) 1TBP18 immunostaining showing the expression of mutant TBP in nestin-TBP knock-in mouse (12 months old) brains. 1TBP18 at the same concentration did not label the control (heterozygous floxed mouse without Cre) mouse (12 months old) brain. Transgenic TBP was detected in the cerebral cortex (Ctx) and striatum (Stra), but not in white matter (WM) of nestin-TBP knock-in mice. Mutant TBP was also present in the molecular, granule and Purkinje layers of the cerebellum in a nestin-TBP knock-in mouse. (**B**) High-power magnification (×630) photographs showing that neurons in the cerebral cortex and striatum in nestin-TBP knock-in mice expressed mutant TBP. In the cerebellum, mutant TBP is more abundant in the Purkinje cells than in the granule layer and molecular layer. Arrows indicate small nuclear aggregates in Purkinje cells. Scale bar = 10 μm. KI = knock-in; Q = glutamine.

(Koide *et al*, 1999; Nakamura *et al*., 2001; Rolfs *et al*., 2003). We found that nestin-TBP knock-in mice also displayed age-dependent degeneration of Purkinje cells (Fig. 4A). The loss of Purkinje cells was revealed by immunostaining with an antibody to calbindin, a cellular marker protein for Purkinje cells, in old nestin-TBP knock-in mice (16 and 23 months), but not in young nestin-TBP knock-in mice at 3 months of age. Higher magnification micrographs could reveal the degeneration of Purkinje cell processes in nestin-TBP knock-in mice at 12 months of age (Supplementary Fig. 1B). To more quantitatively assess this degeneration, we performed western blotting and verified the reduction of calbindin in old nestin-TBP knock-in mouse cerebellum (Fig. 4B). Taken together, mutant TBP, when expressed at the endogenous level in neuronal cells, can also cause age-dependent neurological symptoms and neurodegeneration.

Mutant TBP binds more tightly to nuclear factor-Y

Although our earlier study showed that mutant TBP reduces the expression of the chaperone Hsp25 (Friedman *et al*., 2007),

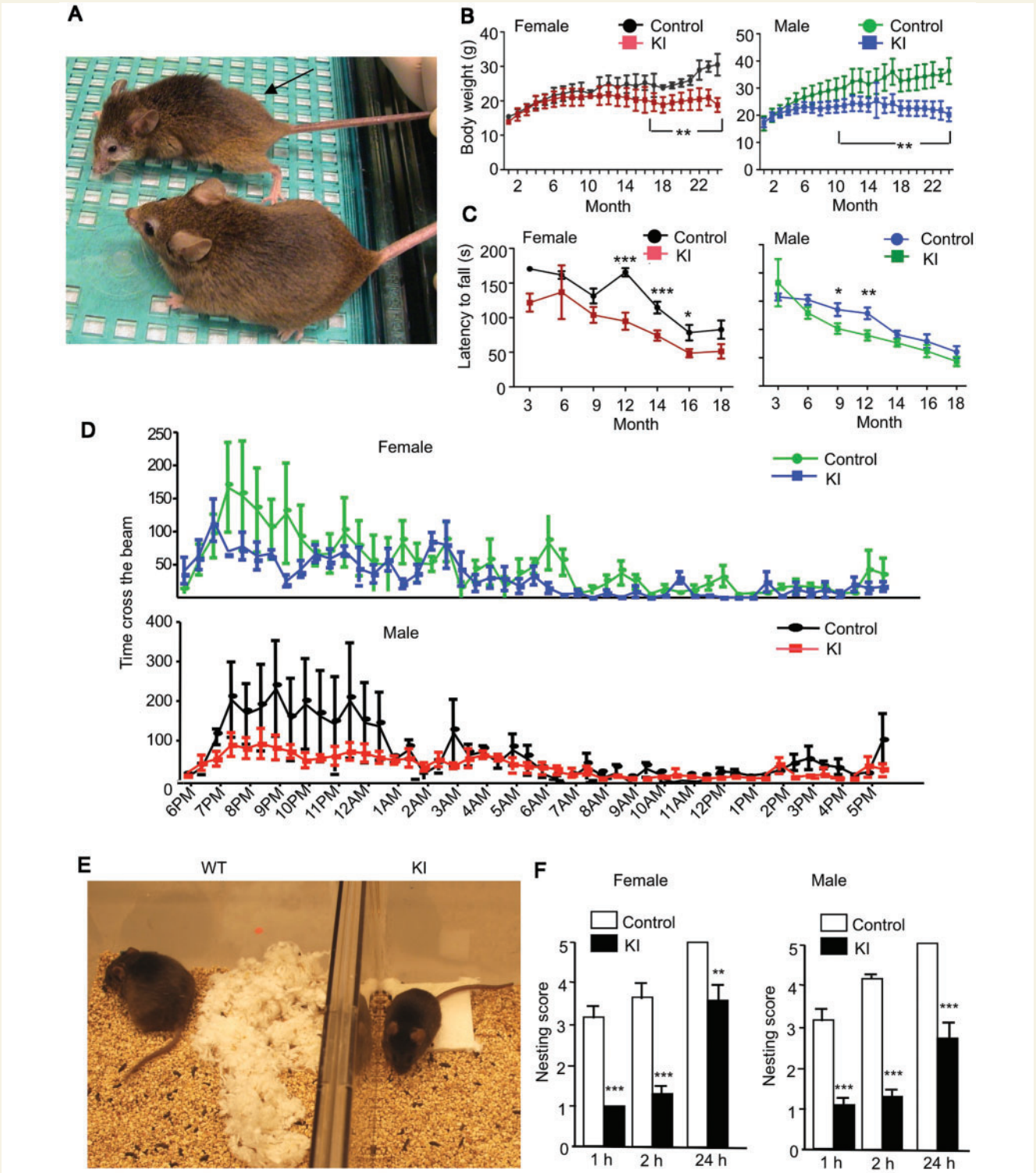

Figure 3 Neurological phenotype of nestin-TBP knock-in mice. (**A**) Nestin-TBP knock-in (KI) mouse (arrow) at 23 months of age was smaller and poorly groomed relative to wild-type (WT) littermates. (**B**) Changes in body weight of female and male nestin-TBP knock-in mice compared with control mice (heterozygous floxed mice without Cre or nestin-Cre mice, $n = 10$ for each group). $^{**}P < 0.01$ compared with control. (**C**) Non-accelerating rotarod (15 rpm) performance of nestin-TBP knock-in mice and age-matched control mice ($n = 10$ for each group). $^{*}P < 0.05$, $^{**}P < 0.01$, $^{***}P < 0.001$ compare with control. (**D**) Locomotor activity over 24 h of nestin-TBP knock-in mice and control mice ($n = 10$ for each group) at the age of 13 months. (**E**) Nestin-TBP knock-in mouse at 18 months of age showing no nest-building behaviour during 12 h examination compared with the control littermate. (**F**) Quantitation of nest-building performance at 1, 2 and 24 h for nestin-TBP knock-in and control mice ($n = 10$ for each group) at the age of 18 months. Nest-building scores were obtained by measuring the nest quality on a scale of 1 (the worst) to 5 (the best) as described in the 'Materials and methods' section. $^{**}P < 0.01$; $^{***}P < 0.001$, compared with control.

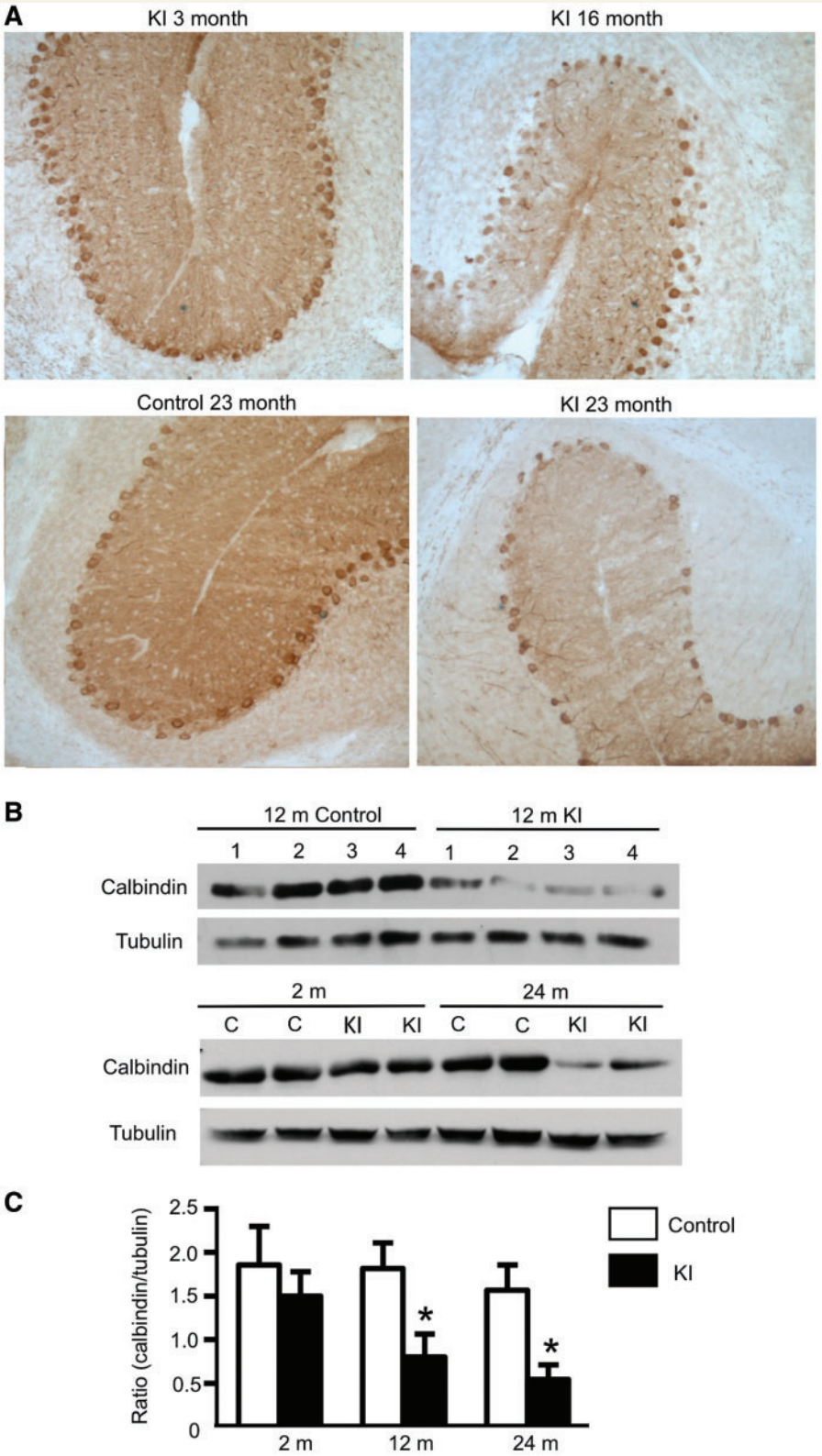

Figure 4 Neurodegeneration in nestin-TBP knock-in mice. (**A**) Representative micrographs of calbindin immunostaining of Purkinje cells in the cerebellum of nestin-TBP knock-in (KI) and control mice. Ages are indicated. (**B**) Western blot analysis of calbindin in cerebellar tissues of 2-, 12-, and 24-month-old nestin-TBP knock-in and control mice (heterozygous floxed mice without Cre or nestin-Cre mice). (**C**) The densitometric ratios of calbindin to tubulin are also included. $*P < 0.05$ compared with control.

the mechanism underlying this phenomenon remained to be investigated. We examined several transcription factors that interact with TBP and found that nuclear factor-Y, also termed CCAAT box-binding factor (CBF) (Mantovani, 1999; Matuoka and Chen, 2002), colocalized with nuclear TBP inclusions in the cerebellum of SCA17 transgenic mice (Fig. 5A). Nuclear factor-Y is a heterotrimeric complex that consists of three subunits, nuclear factor-YA, nuclear factor-YB and nuclear factor-YC, and binds to TBP (Bellorini *et al*., 1997; Kotova *et al*., 2001; Fang *et al*., 2004) and CCAAT motifs in the promoter regions of a variety of genes (Mantovani, 1999; Matuoka and Chen, 2002). We chose to focus on nuclear factor-YA, as its available antibody allows for western blotting and immunocytochemistry analysis. Our first step to establish an association was to examine the cerebellum of SCA17 transgenic mice that show obvious nuclear inclusions formed by overexpressed TBP in cerebellar granule cells (Friedman *et al*., 2007). The colocalization of nuclear factor-YA with TBP nuclear aggregates is evident in the cerebellum of SCA17 transgenic mice (Fig. 5A). We also examined cultured cerebellar granule cells from transgenic SCA17 mice, as these granule cells show abundant nuclear aggregates (Friedman *et al*., 2007). We found a clear localization of nuclear factor-YA in the nuclear inclusions of mutant cerebellar granule cells (Fig. 5B). To provide more direct evidence for the association between mutant TBP aggregates and nuclear factor-YA, we transfected mutant TBP and nuclear factor-YA into HEK293 cells and then examined their localization. While nuclear factor-YA was distributed diffusely in the nucleus in the absence of mutant TBP, it became colocalized with nuclear aggregates when mutant TBP was also present (Fig. 5C). All of these findings provide strong evidence for the association of nuclear factor-YA with aggregated TBP.

To examine whether nuclear factor-YA also associates with soluble mutant TBP, we performed biochemical assays of the direct interaction between GST-TBP and *in vitro* translated nuclear factor-YA and found that more nuclear factor-YA was pulled down by GST-TBP-71-glutamine than GST-TBP-13-glutamine (Fig. 6A). Cotransfection of nuclear factor-YA with TBP-71-glutamine or TBP-31-glutamine in HEK293 cells also led to more precipitation of soluble TBP-71-glutamine than TBP-31-glutamine in nuclear factor-YA immunoprecipitations (Fig. 6B). These results demonstrate that more nuclear factor-YA binds soluble mutant TBP in GST pulldown and immunoprecipitation. In addition, aggregated TBP was immunoprecipitated with nuclear factor-YA, consistent with the colocalization of mutant TBP aggregates with nuclear factor-YA seen in Fig. 5. Using anti-TBP for immunoprecipitation of brain cerebellar extracts from control and nestin-TBP knock-in mice, we also saw that more nuclear factor-YA was precipitated from nestin-TBP knock-in mouse brain (Fig. 6C), indicating that more nuclear factor-YA binds mutant TBP in the mouse brain.

Mutant TBP inhibits nuclear factor-YA transcriptional activity

To provide evidence that the abnormal interaction of mutant TBP with nuclear factor-YA can affect the transcriptional activity of nuclear factor-YA, we generated luciferase reporter DNA constructs driven either by the proximal promoter or only the CCAAT binding sites in the minimal promoter region for human HSP27, which is equivalent to mouse Hsp25. Cotransfection of these reporters with nuclear factor-YA into HEK293 cells clearly revealed that nuclear factor-YA could promote the expression of luciferase significantly (Fig. 7A, Supplementary Fig. 2), suggesting that nuclear factor-YA binds the HSP27 promoter to activate the expression of luciferase. Importantly, in the presence of mutant TBP-105-glutamine, there was a significant reduction in this transcriptional activity compared with coexpression with normal TBP-13-glutamine (Fig. 7A). Furthermore, in the reporter assay with the minimal HSP27 promoter that contains only the CCAAT binding site, decreased promoter activity was more evident in the presence of mutant TBP (Fig. 7B). To further investigate whether mutant TBP reduces the association of nuclear factor-YA with the HSP27 promoter via its abnormal interaction with nuclear factor-YA, we performed chromatin immunoprecipitation assays of HEK293 cells that were transfected with either normal human TBP-13-glutamine or mutant TBP-105-glutamine. In the presence of mutant TBP, there was a decrease in the association of nuclear factor-YA with the endogenous HSP27 promoter in HEK293 cells compared with the actin promoter (Fig. 7C and D). Combined with our immunocytochemical and biochemical results showing that mutant TBP binds more tightly to nuclear factor-YA than wild-type TBP, we suspect that mutant TBP is likely to reduce the association of nuclear factor-YA with the chaperone promoter, leading to the decreased levels of HSP27.

Reduced chaperone protein levels in the brain of nestin-TBP knock-in mice

Although nuclear factor-Y is known to mediate the expression of various chaperones, its expression in the brain region in relation to chaperones remains unclear. We found that nuclear factor-YA and mouse Hsp25 are expressed at higher levels in the mouse cerebellum than in the cortex and striatum (Fig. 8A and B). These results suggest that the dysfunction of nuclear factor-YA may have more impact on cerebellar function, leading us to examine the expression of several chaperones in the cerebellum of nestin-TBP knock-in mice. We focused on those chaperones whose expression is regulated by nuclear factor-Y (Taira *et al*., 1999; Imbriano *et al*., 2001; Chae *et al*., 2005), such as Hsp70, which is upregulated by heat shock stress, and HspA5, which is an endoplasmic reticulum stress protein and is known as the 78-kDa glucose-regulated heat shock protein GRP-78 (Marcus and Green, 1997; Luo *et al*., 2008). We found that Hsp70 and HspA5 levels were decreased in the cerebellum of nestin-TBP knock-in mice at 2 and 12 months (Fig. 8C). Although Hsp25 showed no significant change at 2 months, its level in the cerebellum of nestin-TBP knock-in mice was markedly reduced at 12 months (Fig. 8C and D). In contrast, there was no significant change in the level of nuclear factor-YA in nestin-TBP knock-in cerebellar tissues compared with littermate controls, suggesting that the decreased levels of chaperones are more likely due to the dysfunction of nuclear factor-YA.

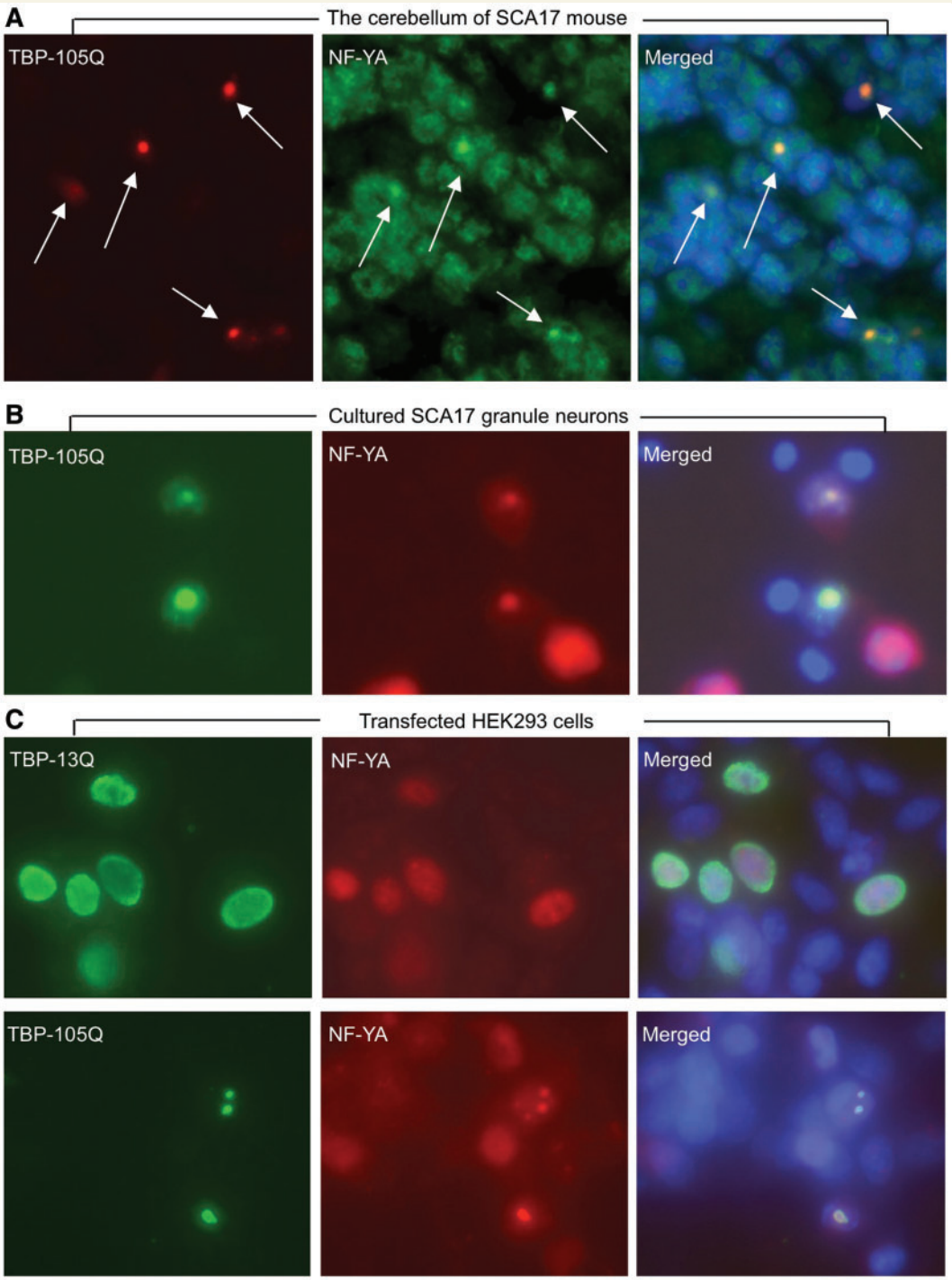

Figure 5 Colocalization of nuclear factor-YA with nuclear TBP inclusions. (**A**) Representative immunofluorescent images showing colocalization of nuclear factor-YA (green) with neuronal nuclear TBP (red) inclusions (arrows) in the transgenic TBP-105-glutamine mouse cerebellum at 3 months of age. The merged image also displays nuclear staining (blue). (**B**) Immunofluorescent staining of cultured cerebellar granule cells from TBP-105-glutamine transgenic mouse with antibodies to TBP (green) and nuclear factor-YA (red). (**C**) Immunofluorescent images showing that transfected nuclear factor-YA (red) colocalized with transfected TBP-105-glutamine (green) aggregates in the nuclei of transfected HEK293 cells. In TBP-13-glutamine and nuclear factor-YA cotransfected HEK293 cells, however, nuclear factor-YA and TBP-13-glutamine were diffused in the nucleus. The merged image displays nuclear staining (blue).
NF-YA = nuclear factor-YA; Q = glutamine.

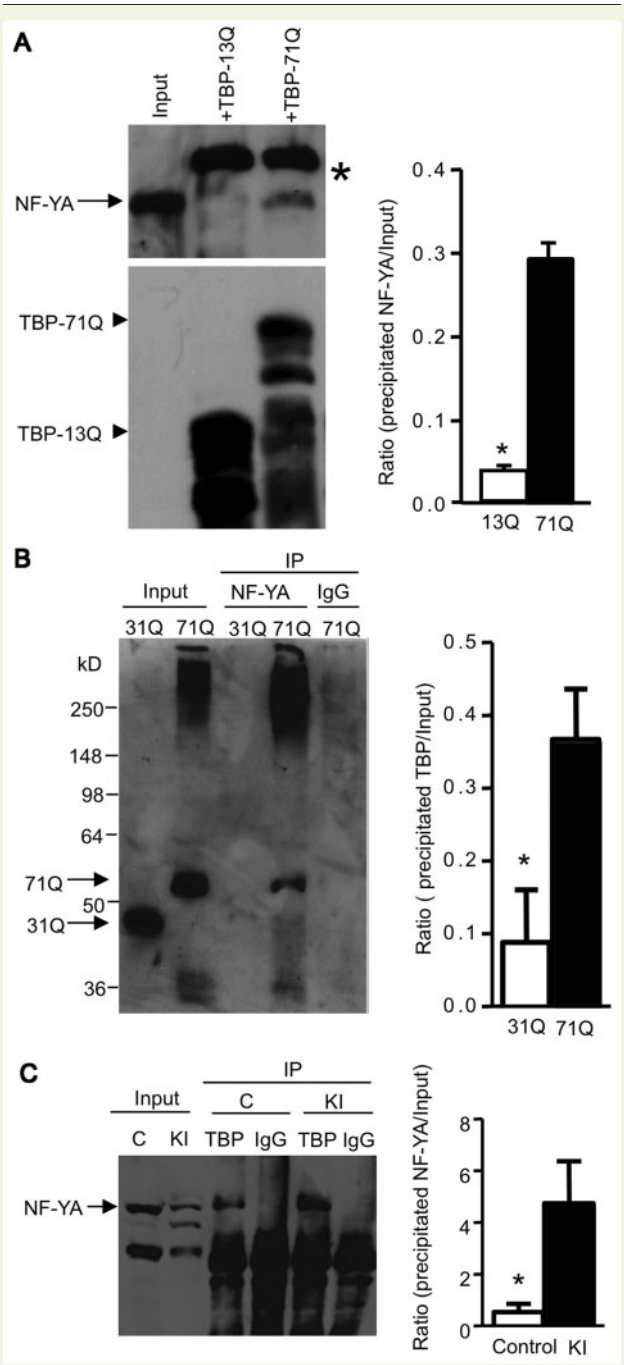

Figure 6 Aberrant interaction of mutant TBP with nuclear factor-YA. (**A**) Representative GST-TBP pulldown assay (*left*) and densitometric analysis (*right*) demonstrating that more *in vitro* synthesized nuclear factor-YA was pulled down by GST-TBP-71-glutamine versus GST-TBP-13-glutamine. Arrow indicates nuclear factor-YA. Star indicates non-specific immunoreactive product. (**B**) Nuclear factor-YA immunoprecipitation (IP) (*left*) of extracts from HEK293 cells cotransfected with nuclear factor-YA and TBP (31-glutamine or 71-glutamine). Densitometric ratio of precipitated TBP to input on the same blot (*right*). The western blot was probed with 1TBP18 antibody. Arrows indicate soluble TBP. (**C**) EM192 (rabbit anti-C-terminal TBP antibody) immunoprecipitation (*left*) of the mouse cerebellar lysates showing coprecipitation of more nuclear factor-YA (arrow) with TBP in nestin-TBP knock-in than in control mice. Control also included precipitation with purified rabbit IgG. The western blot was probed with an antibody to nuclear factor-YA. Mice at 2 months of age were used. (*Right*) Densitometric ratio of precipitated nuclear factor-YA to input on the same blot. $*P < 0.05$ ($n = 3$) compared with 71-glutamine or knock-in. KI = knock-in; NF-YA = nuclear factor-YA; Q = glutamine.

If mutant TBP binds more tightly to nuclear factor-YA and affects its function, we should see an impaired response of the chaperones to stress. To test this hypothesis, we first examined the expression of Hsp25 and Hsp70 in PC12 cell lines that express either normal TBP (13-glutamine) or mutant TBP (105-glutamine). These cells were treated with heat shock for 45 min. The expression of Hsp25 and Hsp70 was then examined 4, 8 and 16 h later, and there was a significant increase of Hsp25 and Hsp70 in the control cells (13-glutamine). In mutant cells expressing polyglutamine-expanded TBP (105-glutamine), however, the levels of Hsp25 and Hsp70 slightly increased or remained unchanged (Fig. 9A). To examine the level of HspA5, which is upregulated by endoplasmic reticulum stress or H_2O_2 (Pan *et al.*, 2010), we treated PC12 cell lines with H_2O_2 at various doses (50, 100, 250 μM). HspA5 was apparently increased after H_2O_2 treatment in control PC12 cells, but not in mutant PC12 cells expressing TBP-105-glutamine (Fig. 9B). To verify that the defect in stress response also occurs *in vivo*, we treated nestin-TBP knock-in mice at 2 months of age with heat shock at 42°C for 45 min. The mice were then recovered for 16 h, and their cerebellar tissues were isolated for western blotting. The results showed that Hsp25 and Hsp70 were increased in the control mice; however, in the cerebellar tissues from nestin-TBP knock-in mice, there was no significant change in Hsp25 and Hsp70 after heat shock (Fig. 9C). To verify that mutant TBP impairs the chaperone response by affecting the function of nuclear factor-Y, we transfected TBP-105-glutamine PC12 cells with nuclear factor-YA and then tested chaperone levels in these cells after heat shock for 45 min. Expression of nuclear factor-YA clearly restored the increase levels of Hsp70 and Hsp25 in response to heat shock (Fig. 9D). Thus, both *in vitro* and *in vivo* experiments, as well as the rescue experiment, demonstrated that mutant TBP caused impairment in the stress response of chaperones.

Discussion

By establishing a mouse model that expresses one copy of the mutant TBP gene in neuronal cells at the endogenous level, we have shown that neuronal mutant TBP mediates age-dependent neurological phenotypes, affects the transcriptional activity of nuclear factor-Y, and reduces the levels of several chaperones. These findings provide new insight into the pathogenesis of SCA17.

Our early transgenic SCA17 mouse model, which overexpresses mutant TBP in neuronal cells by the prion promoter, develops more progressive and more severe neurological phenotypes than nestin-TBP knock-in mice. Similarly, transgenic mice (N171-82Q)

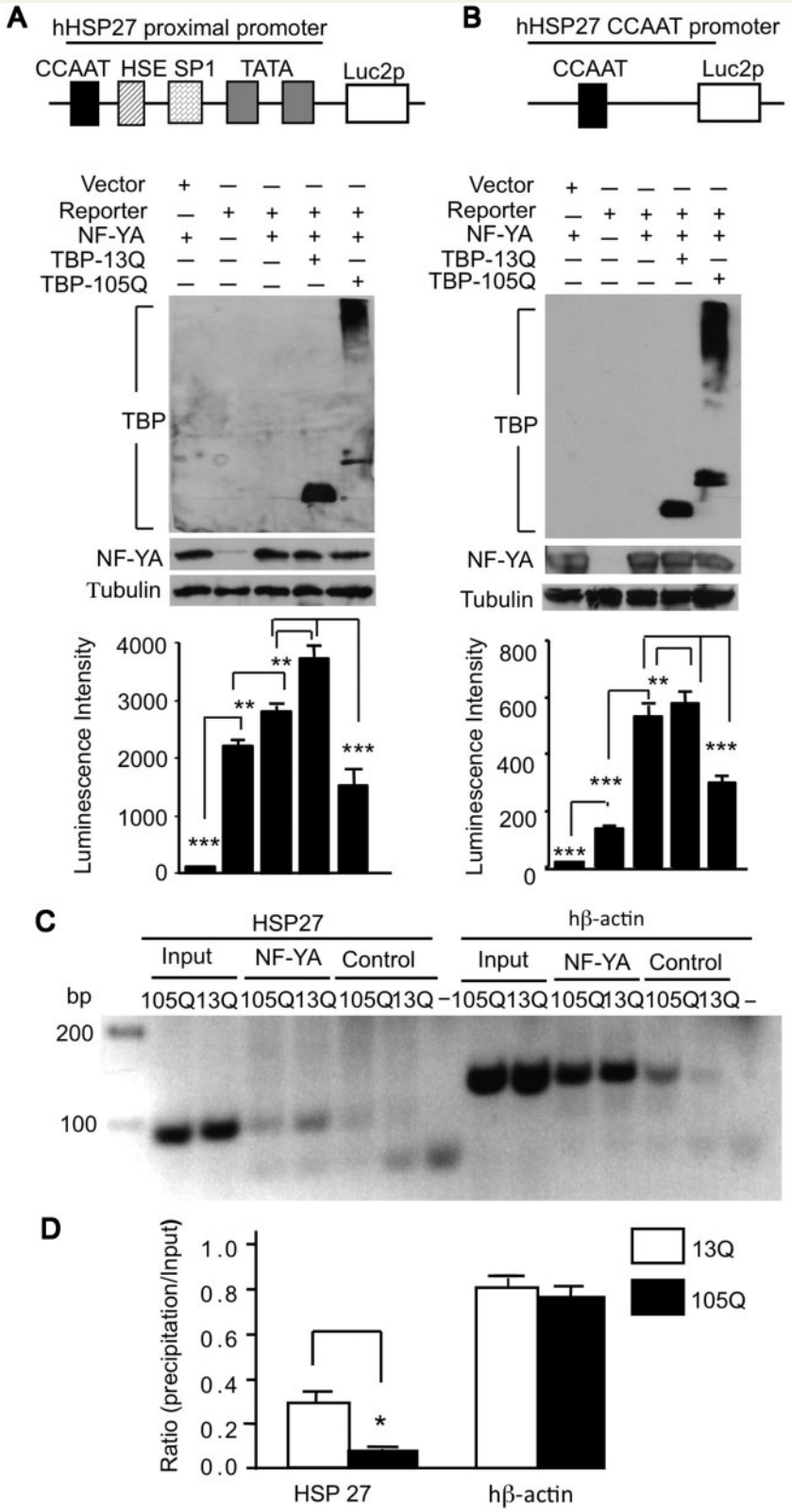

Figure 7 Mutant TBP inhibits the activity of HSP27 promoter and reduces its association with nuclear factor-YA. (**A**) The luciferase reporter under the control of the promoter of human HSP27, which is equivalent to mouse Hsp25 and consists of CCAAT, heat shock responsive elements (HSE), SP1 and TATA binding sites (*upper*), was cotransfected with nuclear factor-YA and TBP into HEK293 cells. Western blotting analysis confirmed the expression of transfected TBP (TBP-13-glutamine and TBP-105-glutamine) and nuclear factor-YA (*middle*). Luciferase expression was quantified as luminescence intensity in transfected cells (*lower*). (**B**) The minimal promoter region containing only the CCAAT binding site in the human HSP27 DNA was used for the luciferase reporter assay. Data are presented in

(continued)

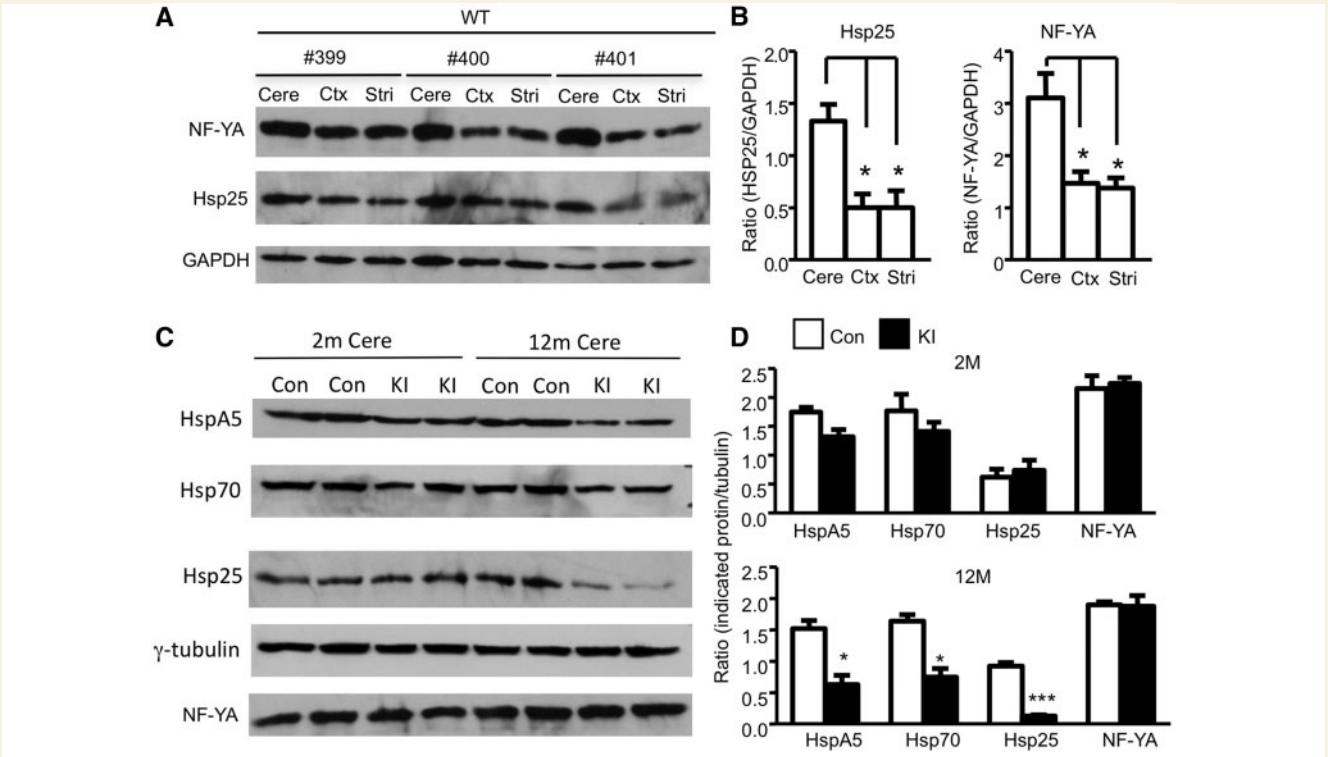

Figure 8 Reduced expression of chaperones in the cerebellum of nestin-TBP knock-in mice. (**A**) Western blotting revealed that nuclear factor-YA and Hsp25 are correlatively higher in the cerebellum (Cere) than in the cortex (Ctx) and striatum (Stri) in three (#399, #400, #401) wild-type (WT) mice. (**B**) The ratios of nuclear factor-YA (NF-YA) and Hsp25 to GAPDH in different mouse brain regions. (**C**) Western blot analysis of the cerebellar tissues of control (Con) (heterozygous floxed mice without Cre or nestin-Cre mice) and nestin-TBP knock-in (KI) mice at 2 and 12 months (m) of age. There is a decrease in HspA5, Hsp70, and Hsp25 in nestin-TBP knock-in mouse cerebellum as compared with tubulin and nuclear factor-YA. (**D**) The ratios of the examined proteins to tubulin are presented (*right*). $^{*}P < 0.05$; $^{***}P < 0.001$.

expressing N-terminal mutant huntingtin by the same prion promoter also show more severe phenotypes than many other Huntington's disease models (Schilling *et al*., 1999; Menalled and Chesselet, 2002; Heng *et al*., 2008). By comparing the transcriptional levels of transgenes in different Huntington's disease mouse models, we have found that the prion promoter mediates the highest level of transgenic huntingtin (Wang *et al.,* 2008). The different extents of the neurological phenotypes in nestin-TBP knock-in versus previously generated transgenic SCA17 mice indicate clearly that the expression levels of polyglutamine proteins determine the nature and severity of neurological phenotypes. Thus, it is important to establish a mouse model that expresses mutant TBP at the endogenous level if we wish to examine SCA17 neuropathology and pathogenesis.

A conditional knock-in approach using the LoxP-Cre system allowed us to generate our new mouse model, which can selectively express mutant TBP in neuronal cells under the endogenous mouse TBP promoter. The findings from this mouse model led to the following implications. First, a gain of toxic function from polyglutamine expansion is probably more important for the development of neuropathology. This is because heterozygous floxed mice without expression of mutant TBP are equivalent to heterozygous TBP knockout mice and do not show neurological phenotypes. Only when Cre is expressed to turn on the expression of mutant TBP in these heterozygous floxed mice did we observe age-dependent neurological phenotypes. Secondly, like other polyglutamine knock-in mice, the phenotypes of nestin-TBP knock-in mice are relatively mild compared with transgenic

Figure 7 Continued
the same manner as for (**A**). $^{**}P < 0.01$; $^{***}P < 0.001$. (**C**) Chromatin immunoprecipitation assay of the association of nuclear factor-YA with the human HSP27 promoter in transfected HEK293 cells that express either normal TBP (13-glutamine) or mutant TBP (105-glutamine). Cross-linked chromatin materials were precipitated by anti-nuclear factor-YA and were subjected to polymerase chain reaction with primers for the promoter region of human HSP27 or β-actin. The polymerase chain reaction products were then revealed by agarose gel electrophoresis. (**D**) Quantitation of chromatin immunoprecipitation assay by measuring the ratios of precipitated polymerase chain reaction products to the input. $^{*}P < 0.05$ ($n = 3$). NF-YA = nuclear factor-YA; Q = glutamine.

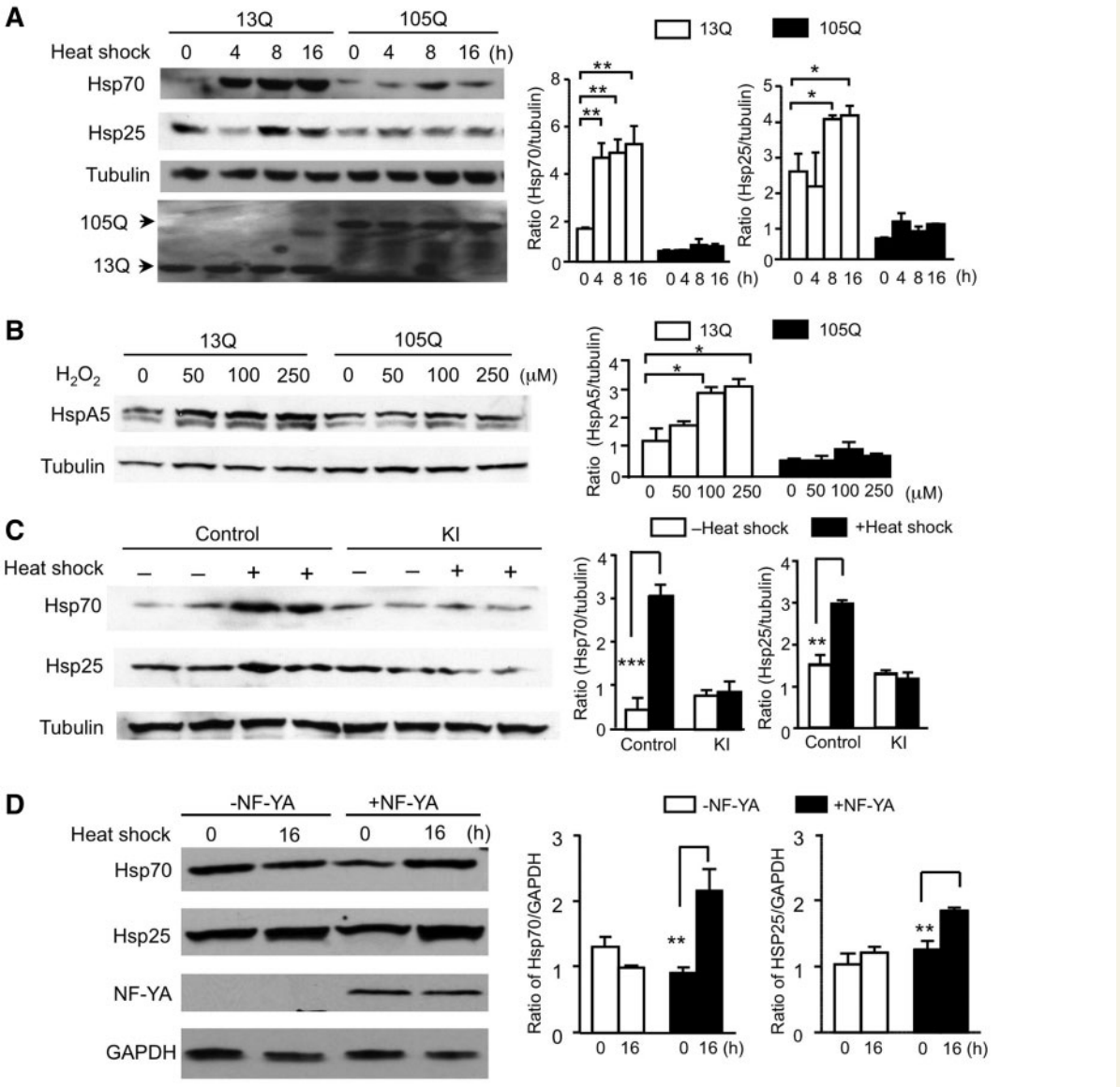

Figure 9 Mutant TBP impairs stress response of chaperones. (**A**) Western blot analysis of PC12 cells expressing TBP-13-glutamine or TBP-105-glutamine. The cells were treated with heat shock at 42°C for 45 min and then examined at 4, 8 and 16 h after heat shock. Increased levels of Hsp70 and Hsp25 were seen in the control cells (13-glutamine), but not in mutant cells (105-glutamine). (*Right*) Ratios of Hsp70 and Hsp25 to tubulin are presented. (**B**) To examine HspA5's response to stress, the PC12 cells were treated with H_2O_2 at 50, 100 and 250 μM for 4 h. Western blotting revealed that HspA5 was not increased in mutant PC12 cells (105-glutamine) compared with control cells (13-glutamine). Ratio of HspA5 is shown on the *right*. (**C**) Control (heterozygous floxed mice without Cre or nestin-Cre mice) and nestin-TBP knock-in (KI) mice at 2 months of age were treated with heat shock for 45 min. Mouse cerebellar tissue extracts were then isolated 16 h later for western blot analysis. Note that control cerebellar lysates show increased levels of Hsp70 and Hsp25, while nestin-TBP knock-in samples fail to show this increase. Ratios of Hsp70 and Hsp25 to tubulin are also presented (*right*). (**D**) TBP-105-glutamine PC12 cells were transfected with (+) or without (−) nuclear factor-YA and then treated with heat shock at 42°C for 45 min. The lysates of cells were analysed via western blotting (*left*) to examine the expression of Hsp70 and Hsp25 16 h after heat shock. The ratios of Hsp70 or Hsp25 to GAPDH were also presented (*right*). $^*P < 0.05$; $^{**}P < 0.01$; $^{***}P < 0.001$. KI = knock-in; NF-YA = nuclear factor-YA; Q = glutamine.

SCA17 mice that overexpress mutant proteins. Thus, regardless of the critical function of TBP or non-essential function of other polyglutamine proteins, the expression of mutant polyglutamine proteins at the endogenous level appears to cause only slow and mild phenotypes in mice. This phenomenon is in keeping with the idea that expanded polyglutamine creates a toxic function that is age-dependent. Thirdly, neuronal expression of polyglutamine proteins at the endogenous level can cause neurodegeneration. Given the mounting evidence for pathology caused by non-neuronal polyglutamine proteins or non-autonomous mechanisms (Bradford *et al*., 2009, 2010; Sassone *et al*., 2009; van der Burg *et al*., 2009), it is very likely that the combined effects of

mutant proteins in various types of cells determine the severity and specificity of neurodegeneration in polyglutamine diseases.

It is conceivable that abnormal protein interactions caused by polyglutamine expansion lead to multiple pathological pathways including transcriptional dysregulation (Havel *et al*., 2009). Unlike huntingtin and other polyglutamine proteins, TBP is a well-characterized transcription factor that is predominantly localized in the nucleus; thus, the toxicity of mutant TBP is likely to occur predominantly in the nucleus. Although TBP associates with a variety of transcription factors to regulate the expression of the vast majority of genes, our early studies of transgenic SCA17 mice using Affymetrix microarrays revealed no overt abnormalities of transcriptional profiling in the brains of these mutant mice (Friedman *et al*., 2007), suggesting that polyglutamine expansion may selectively affect the function of specific transcription factors and their targets. The abnormal interaction of mutant TBP with nuclear factor-YA is reminiscent of the abnormal association of mutant huntingtin with nuclear factor-Y (Yamanaka *et al*., 2008) and the colocalization of polyglutamine-expanded androgen receptor aggregates with nuclear factor-Y (Katsuno *et al*., 2010). Nuclear factor-Y binds CCAAT sequences and promotes the expression of a variety of genes, including those for chaperones (Taira *et al*., 1999; Imbriano *et al*., 2001; Chae *et al*., 2005). As the regulation of chaperone expression also depends on other transcription factors, the selectivity of the influences of mutant TBP on chaperone transcription is likely to be determined by those transcription factors or regulators that form the same or independent protein complexes with nuclear factor-Y and/or TBP during the transcription activation process (Bellorini *et al*., 1997; Frontini *et al*., 2002; Zhao *et al*., 2003). For example, nuclear factor-Y also directly interacts with Sp1 (Roder *et al*., 1999), which is found to bind abnormally to mutant TBP (Friedman *et al*., 2008) and huntingtin (Dunah *et al*., 2002; Li *et al*., 2002). Decreased Hsp70 was also evident in Huntington's disease mouse brain tissues (Hay *et al*., 2004; Orr *et al*., 2008; Yamanaka *et al*., 2008), and the neurological phenotypes and pathology of Huntington's disease and SCA17 were also similar. The dysfunction of nuclear factor-YA and the impairment of chaperone response seen in our SCA17 cellular and mouse models could be a common pathogenic pathway shared by both Huntington's disease and SCA17, and perhaps by other polyglutamine diseases as well.

Uncovering the negative impact of mutant TBP on chaperone expression also gives us a new direction to further explore the shared pathogenesis of Huntington's disease and SCA17, as well as their treatment. Chaperones are known to be protective against neuronal damage under cellular stress (Kalmar and Greensmith, 2009), and acute and chronic stress can occur to neuronal cells in the brain over the course of ageing. Reduced levels of chaperones in the brain would decrease the cellular capacity to refold polyglutamine proteins and to protect against oxidative stress during ageing, which can promote ageing-related neuropathological changes. Although improving chaperone function in neuronal cells has been proposed to reduce the toxicity of misfolded proteins (Williams and Paulson, 2008; Arawaka *et al*., 2010; Sajjad *et al*., 2010), the complexity of chaperones has made it difficult to pinpoint specific targets for effective treatment. Thus, identifying the role of nuclear factor-YA dysfunction in polyglutamine protein-mediated toxicity could help us develop a new therapeutic approach to SCA17. Our current findings should also be helpful in the quest to alleviate the neuropathology associated with mutant huntingtin and other polyglutamine proteins.

Acknowledgements

We thank Karthik Ponnapula for technical assistance and Cheryl Strauss for critical reading of the manuscript.

Funding

United States National Institutes of Health grant (AG019206 and NS041669, to X.-J.L.; and AG031153 and NS045016, to S.L.).

Supplementary material

Supplementary material is available at *Brain* online.

References

Arawaka S, Machiya Y, Kato T. Heat shock proteins as suppressors of accumulation of toxic prefibrillar intermediates and misfolded proteins in neurodegenerative diseases. Curr Pharm Biotechnol 2010; 11: 158–66.

Ballard TM, Pauly-Evers M, Higgins GA, Ouagazzal AM, Mutel V, Borroni E, et al. Severe impairment of NMDA receptor function in mice carrying targeted point mutations in the glycine binding site results in drug-resistant nonhabituating hyperactivity. J Neurosci 2002; 22: 6713–23.

Bauer P, Laccone F, Rolfs A, Wullner U, Bosch S, Peters H, et al. Trinucleotide repeat expansion in SCA17/TBP in white patients with Huntington's disease-like phenotype. J Med Genet 2004; 4: 230–2.

Bellorini M, Lee DK, Dantonel JC, Zemzoumi K, Roeder RG, Tora L, et al. CCAAT binding NF-Y-TBP interactions: NF-YB and NF-YC require short domains adjacent to their histone fold motifs for association with TBP basic residues. Nucleic Acids Res 1997; 25: 2174–81.

Bradford J, Shin JY, Roberts M, Wang CE, Li XJ, Li S. Expression of mutant huntingtin in mouse brain astrocytes causes age-dependent neurological symptoms. Proc Natl Acad Sci USA 2009; 106: 22480–5.

Bradford JW, Li S, Li XJ. Polyglutamine toxicity in non-neuronal cells. Cell Res 2010; 20: 400–7.

Bruni AC, Takahashi-Fujigasaki J, Maltecca F, Foncin JF, Servadio A, Casari G, et al. Behavioral disorder, dementia, ataxia, and rigidity in a large family with TATA box-binding protein mutation. Arch Neurol 2004; 61: 1314–20.

Chae HD, Yun J, Shi DY. Transcription repression of a CCAAT-binding transcription factor CBF/HSP70 by p53. Exp Mol Med 2005; 37: 488–91.

Dunah AW, Jeong H, Griffin A, Kim YM, Standaert DG, Hersch SM, et al. Sp1 and TAFII130 transcriptional activity disrupted in early Huntington's disease. Science 2002; 296: 2238–43.

Duvick L, Barnes J, Ebner B, Agrawal S, Andresen M, Lim J, et al. SCA1-like disease in mice expressing wild-type ataxin-1 with a serine to aspartic acid replacement at residue 776. Neuron 2010; 67: 929–35.

Fang X, Han H, Stamatoyannopoulos G, Li Q. Developmentally specific role of the CCAAT box in regulation of human gamma-globin gene expression. J Biol Chem 2004; 279: 5444–9.

Friedman MJ, Shah AG, Fang ZH, Ward EG, Warren ST, Li S, et al. Polyglutamine domain modulates the TBP-TFIIB interaction: implications for its normal function and neurodegeneration. Nat Neurosci 2007; 10: 1519–28.

Friedman MJ, Wang CE, Li XJ, Li S. Polyglutamine expansion reduces the association of TATA-binding protein with DNA and induces DNA binding-independent neurotoxicity. J Biol Chem 2008; 283: 8283–90.

Frontini M, Imbriano C, diSilvio A, Bell B, Bogni A, Romier C, et al. NF-Y recruitment of TFIID, multiple interactions with histone fold TAF(II)s. J Biol Chem 2002; 277: 5841–8.

Havel LS, Li S, Li X-J. Nuclear accumulation of polyglutamine disease proteins and neuropathology. Mol Brain 2009; 2: 21.

Hay DG, Sathasivam K, Tobaben S, Stahl B, Marber M, Mestril R, et al. Progressive decrease in chaperone protein levels in a mouse model of Huntington's disease and induction of stress proteins as a therapeutic approach. Hum Mol Genet 2004; 13: 1389–405.

Heng MY, Detloff PJ, Albin RL. Rodent genetic models of Huntington disease. Neurobiol Dis 2008; 32: 1–9.

Hu Y, Metzler B, Xu Q. Discordant activation of stress-activated protein kinases or c-Jun NH2-terminal protein kinases in tissues of heat-stressed mice. J Biol Chem 1997; 272: 9113–9.

Imbriano C, Bolognese F, Gurtner A, Piaggio G, Mantovani R. HSP-CBF is an NF-Y-dependent coactivator of the heat shock promoters CCAAT boxes. J Biol Chem 2001; 276: 26332–9.

Kalmar B, Greensmith L. Induction of heat shock proteins for protection against oxidative stress. Adv Drug Deliv Rev 2009; 61: 310–8.

Katsuno M, Adachi H, Minamiyama M, Waza M, Doi H, Kondo N, et al. Disrupted transforming growth factor-beta signaling in spinal and bulbar muscular atrophy. J Neurosci 2010; 30: 5702–12.

Koide R, Kobayashi S, Shimohata T, Ikeuchi T, Maruyama M, Saito M, et al. A neurological disease caused by an expanded CAG trinucleotide repeat in the TATA-binding protein gene: a new polyglutamine disease? Hum Mol Genet 1999; 8: 2047–53.

Kotova I, Chabes AL, Segerman B, Flodell S, Thelander L, Bjorklund S. A mouse in vitro transcription system reconstituted from highly purified RNA polymerase II, TFIIH and recombinant TBP, TFIIB, TFIIE and TFIIF. Eur J Biochem 2001; 268: 4527–36.

Li SH, Cheng AL, Zhou H, Lam S, Rao M, Li H, et al. Interaction of Huntington disease protein with transcriptional activator Sp1. Mol Cell Biol 2002; 22: 1277–87.

Lijam N, Paylor R, McDonald MP, Crawley JN, Deng CX, Herrup K, et al. Social interaction and sensorimotor gating abnormalities in mice lacking Dvl1. Cell 1997; 90: 895–905.

Long JM, LaPorte P, Paylor R, Wynshaw-Boris A. Expanded characterization of the social interaction abnormalities in mice lacking Dvl1. Genes Brain Behav 2004; 3: 51–62.

Luo R, Lu JF, Hu Q, Maity SN. CBF/NF-Y controls endoplasmic reticulum stress induced transcription through recruitment of both ATF6(N) and TBP. J Cell Biochem 2008; 104: 1708–23.

Mantovani R. The molecular biology of the CCAAT-binding factor NF-Y. Gene 1999; 239: 15–27.

Marcus N, Green M. NF-Y, a CCAAT box-binding protein, is one of the trans-acting factors necessary for the response of the murine ERp72 gene to protein traffic. DNA Cell Biol 1997; 16: 1123–31.

Mariotti C, Alpini D, Fancellu R, Soliveri P, Grisoli M, Ravaglia S, et al. Spinocerebellar ataxia type 17 (SCA17): oculomotor phenotype and clinical characterization of 15 Italian patients. J Neurol 2007; 254: 1538–46.

Martianov I, Viville S, Davidson I. RNA polymerase II transcription in murine cells lacking the TATA binding protein. Science 2002; 298: 1036–9.

Matuoka K, Chen KY. Transcriptional regulation of cellular ageing by the CCAAT box-binding factor CBF/NF-Y. Ageing Res Rev 2002; 1: 639–51.

Menalled LB, Chesselet MF. Mouse models of Huntington's disease. Trends Pharmacol Sci 2002; 23: 32–9.

Moretti P, Bouwknecht JA, Teague R, Paylor R, Zoghbi HY. Abnormalities of social interactions and home-cage behavior in a mouse model of Rett syndrome. Hum Mol Genet 2005; 14: 205–20.

Nakamura K, Jeong SY, Uchihara T, Anno M, Nagashima K, Nagashima T, et al. SCA17, a novel autosomal dominant cerebellar ataxia caused by an expanded polyglutamine in TATA-binding protein. Hum Mol Genet 2001; 10: 1441–8.

Orr AL, Huang S, Roberts MA, Reed JC, Li S, Li XJ. Sex-dependent effect of BAG1 in ameliorating motor deficits of Huntington disease transgenic mice. J Biol Chem 2008; 283: 16027–36.

Orr HT, Zoghbi HY. Trinucleotide repeat disorders. Annu Rev Neurosci 2007; 30: 575–621.

Pan C, Giraldo GS, Prentice H, Wu JY. Taurine protection of PC12 cells against endoplasmic reticulum stress induced by oxidative stress. J Biomed Sci 2010; 17 (Suppl 1): S17.

Roder K, Wolf SS, Larkin KJ, Schweizer M. Interaction between the two ubiquitously expressed transcription factors NF-Y and Sp1. Gene 1999; 234: 61–9.

Rolfs A, Koeppen AH, Bauer I, Bauer P, Buhlmann S, Topka H, et al. Clinical features and neuropathology of autosomal dominant spinocerebellar ataxia (SCA17). Ann Neurol 2003; 54: 367–75.

Sajjad MU, Samson B, Wyttenbach A. Heat shock proteins: therapeutic drug targets for chronic neurodegeneration? Curr Pharm Biotechnol 2010; 11: 198–215.

Sassone J, Colciago C, Cislaghi G, Silani V, Ciammola A. Huntington's disease: the current state of research with peripheral tissues. Exp Neurol 2009; 219: 385–97.

Schilling G, Becher MW, Sharp AH, Jinnah HA, Duan K, Kotzuk JA, et al. Intranuclear inclusions and neuritic aggregates in transgenic mice expressing a mutant N-terminal fragment of huntingtin. Hum Mol Genet 1999; 8: 397–407.

Shah AG, Friedman MJ, Huang S, Roberts M, Li XJ, Li S. Transcriptional dysregulation of TrkA associates with neurodegeneration in spinocerebellar ataxia type 17. Hum Mol Genet 2009; 18: 4141–52.

Sluyter F, Bult A, Lynch CB, van Oortmerssen GA, Koolhaas JM. A comparison between house mouse lines selected for attack latency or nest-building: evidence for a genetic basis of alternative behavioral strategies. Behav Genet 1995; 25: 247–52.

Szczypka MS, Kwok K, Brot MD, Marck BT, Matsumoto AM, Donahue BA, et al. Dopamine production in the caudate putamen restores feeding in dopamine-deficient mice. Neuron 2001; 30: 819–28.

Taira T, Sawai M, Ikeda M, Tamai K, Iguchi-Ariga SM, Ariga H. Cell cycle-dependent switch of up-and down-regulation of human hsp70 gene expression by interaction between c-Myc and CBF/NF-Y. J Biol Chem 1999; 274: 24270–9.

Toyoshima Y, Yamada M, Onodera O, Shimohata M, Inenaga C, Fujita N, et al. SCA17 homozygote showing Huntington's disease-like phenotype. Ann Neurol 2004; 55: 281–6.

Tronche F, Kellendonk C, Kretz O, Gass P, Anlag K, Orban PC, et al. Disruption of the glucocorticoid receptor gene in the nervous system results in reduced anxiety. Nat Genet 1999; 23: 99–103.

van der Burg JM, Bjorkqvist M, Brundin P. Beyond the brain: widespread pathology in Huntington's disease. Lancet Neurol 2009; 8: 765–74.

Wang CE, Tydlacka S, Orr AL, Yang SH, Graham RK, Hayden MR, et al. Accumulation of N-terminal mutant huntingtin in mouse and monkey models implicated as a pathogenic mechanism in Huntington's disease. Hum Mol Genet 2008; 17: 2738–51.

Williams AJ, Paulson HL. Polyglutamine neurodegeneration: protein misfolding revisited. Trends Neurosci 2008; 31: 521–8.

Yamanaka T, Miyazaki H, Oyama F, Kurosawa M, Washizu C, Doi H, et al. Mutant Huntingtin reduces HSP70 expression through the sequestration of NF-Y transcription factor. EMBO J 2008; 27: 827–39.

Zhao J, Bilsland A, Hoare SF, Keith WN. Involvement of NF-Y and Sp1 binding sequences in basal transcription of the human telomerase RNA gene. FEBS Lett 2003; 536: 111–9.

Zühlke CH, Spranger M, Spranger S, Voigt R, Lanz M, Gehlken U, et al. SCA17 caused by homozygous repeat expansion in TBP due to partial isodisomy 6. Eur J Hum Genet 2003; 11: 629–32.